

# SCIENTIFIC REPORTS



OPEN

## Modelling the evolution of transcription factor binding preferences in complex eukaryotes

Antonio Rosanova, Alberto Colliva, Matteo Osella &amp; Michele Caselle

Transcription factors (TFs) exert their regulatory action by binding to DNA with specific sequence preferences. However, different TFs can partially share their binding sequences due to their common evolutionary origin. This “redundancy” of binding defines a way of organizing TFs in “motif families” by grouping TFs with similar binding preferences. Since these ultimately define the TF target genes, the motif family organization entails information about the structure of transcriptional regulation as it has been shaped by evolution. Focusing on the human TF repertoire, we show that a one-parameter evolutionary model of the Birth-Death-Innovation type can explain the TF empirical repartition in motif families, and allows to highlight the relevant evolutionary forces at the origin of this organization. Moreover, the model allows to pinpoint few deviations from the neutral scenario it assumes: three over-expanded families (including HOX and FOX genes), a set of “singleton” TFs for which duplication seems to be selected against, and a higher-than-average rate of diversification of the binding preferences of TFs with a Zinc Finger DNA binding domain. Finally, a comparison of the TF motif family organization in different eukaryotic species suggests an increase of redundancy of binding with organism complexity.

Transcriptional regulation plays a crucial role in most physiological processes, ranging from cell homeostasis to differentiation<sup>1–3</sup>, and its dysregulation is often implicated in pathological processes such as cancer<sup>4</sup>. Mainly thanks to transcriptional regulation, species with highly similar genome sequences can have radically different expression patterns and as a consequence very different phenotypes<sup>5–8</sup>. Therefore, deciphering the mechanisms of evolution of transcriptional regulation is a core part of modern evolutionary biology<sup>9–16</sup>.

Transcriptional regulation is mainly controlled by a class of proteins known as transcription factors (TFs) which are characterized by the presence of at least one DNA binding domain (DBD), i.e., a structural domain able to mediate the TF-DNA interaction. Through this protein-DNA interaction, TFs can recognize their target genes and induce or repress their transcription. The set of TFs with their corresponding targets ultimately define the complex network of regulations that orchestrates the organism gene expression program. Therefore, evolutionary changes in the TF repertoire and/or in their sequence binding preferences can induce large-scale alterations in the gene expression program, thus representing a primary potential source of phenotypic variation and evolution.

Gene duplication and gene loss are main drivers of genome evolution and thus also of the TF repertoire<sup>17–19</sup>. For example, in eukaryotes around the 90% of genes is the result of an event of gene duplication<sup>8,9,20,21</sup>. Moreover, changes in gene copy numbers play a role in evolutionary adaptation comparable to the role of sequence alteration through mutations<sup>19</sup>, and this may be particular true for the evolution along the human lineage<sup>19</sup>, which will be the main focus of this paper. Indeed, gene gain and loss seem to account for a large part of the human/chimpanzee genetic divergence<sup>22,23</sup>. These basic evolutionary moves of duplication and deletion can significantly alter the transcriptional regulatory network by expanding or reducing the number of TFs with certain specific binding preferences. After duplication of a TF gene, the two resulting gene copies are likely redundant. In fact, initially the two TFs share the same sequence, including the DBD sequence that encodes their binding preferences, and thus they also bind to the same target genes. Subsequently, mutations in the DBD sequence can eventually induce one of the TF copies to switch to regulating different target genes<sup>24</sup>, thus resolving the initial redundancy. Alternatively, the regulatory redundancy may be retained to increase the network robustness<sup>25</sup>, or the combinatorial complexity of regulation if the two TFs continue to regulate the same set of target genes but evolve to respond to different cellular signals or to interact with different proteins<sup>18,26</sup>. The organization of TFs in “families” collecting TFs with the same binding preferences, thus putatively TFs with highly overlapping sets of target

Department of Physics and INFN, Università degli Studi di Torino, via P.Giuria 1, I-10125, Turin, Italy. Correspondence and requests for materials should be addressed to A.R. (email: [antonio.rosanova@unito.it](mailto:antonio.rosanova@unito.it))

genes, should carry signatures of the evolutionary forces in action. For example, a duplication event expands a TF family, while the progressive sequence divergence of a TF may give rise to a new TF family able to recognize a significantly different set of target genes. These dynamics could be typically dominated by neutral evolution, but the TF organization may also conceal hallmarks of adaptive selection that, for example, drove the over-expansion of specific TFs or their functional diversification.

The goal of this paper is precisely to design a method to address quantitatively the evolutionary dynamics that shaped the TF repertoire and their TF binding preferences. In order to do so, we first propose a method to organize TFs in families based on their binding preferences that we call “motif families”. Second, we introduce a simple stochastic model of neutral evolution based on the duplication-and-divergence dynamics described above that can be treated analytically and with stochastic simulations. The model introduces a neutral scenario for the distribution of sizes of the TF families able to explain the general empirical repartition of TFs in motif families in human. At the same time, a quantitative theoretical framework allows to pinpoint specific deviations from the neutral expectations that can be the result of selection. The model also introduces a natural measure of TF binding redundancy, and by comparing several eukaryotic model species a striking evolutionary trend can be identified.

## Results

**Organization of TFs in motif families.** Although the number of TFs may vary substantially from genome to genome, the number of distinct DBD types is small. In fact, a previous study<sup>27</sup> distinguishes just barely one hundred sequence-specific DNA-binding domains. The metazoa-specific set of DBDs is limited to a few dozens. Such a classification is perfectly suited to identify long-term patterns of duplication and conservation, but it is too coarse-grained to capture the fine changes in regulation which occur on a much faster evolutionary time scale. Indeed, just a few single-nucleotide mutations in the DBD active site are enough to modify the binding preferences, without a significant change of the DBD structure. To highlight these fine changes of binding preferences a “PWM based” classification of TFs is mandatory. Such a classification was out of reach up to a few years ago, due to the uncertainty in PWM definition (above all for paralogous TFs!), but can be now addressed in a reliable way thanks to the recent experimental and computational progress in PWM reconstruction<sup>27</sup>. Leveraging on this remarkable progress, we propose here a classification of TFs based on their binding preferences, following the approach of Jolma *et al.*<sup>28</sup>. The result of this classification is an organization of TFs in what we call *motif families*, which group together TFs associated to the same PWM (see below for a more precise definition). This organization in motif families is a sub-partition of the DBD classification, which is expected to be more closely related to the TF regulatory potential and thus to evolutionary forces which shaped the regulatory network. This paper proposes a model of the evolutionary process at the origin of this TF organization, which is essentially the following. After a duplication event, TFs in the same DBD class are in the same motif family. Mutations may drive a TF out of its motif family, giving rise to a new motif family, but remaining in the same DBD one.

We based our analysis on the PWM classification proposed in a previous work<sup>27</sup>. In this classification, each TF is associated to a set of PWMs obtained with different experimental techniques or inferred on the basis of DBD homology<sup>27</sup>. This homology-based inference allows to associate a PWM experimentally found for a specific TF to other TFs in the same DBD class that show a particularly high homology in the DNA binding domain<sup>27</sup>. In principle, one could combine these different PWMs to construct a single comprehensive PWM for each TF, but the different methods used to obtain them (with different resolution power) suggest to avoid this merging procedure. Instead, the PWM/TF association can be represented as a bipartite network with two classes of nodes (TFs and PWMs) and links between TFs and PWMs if they are associated in the CIS-BP database. By construction, in this network there are no direct links between PWMs. It is easy at this point to construct the “TF projection” of this bipartite network, which is composed only by the TF nodes with links connecting two TFs if they are associated to at least one common PWM. The network defined in this way is characterized by several disconnected components of high link density, each of which defines a motif family (Fig. 1). Most of these components are cliques, i.e., groups of TFs with at least one PWM in common among all the members. Figure 1 shows that most of the DBDs families are split in smaller more specific motif families. The “splitting rule” turns out not to be uniform, as some DBD classes appear more inclined to diverge than others. Three examples of the splitting of DBD families in motif families are discussed in detail in Section 5 of the Supplementary Material. Figure 2 reports the size distribution of motif families. It is worth noting the large number of motif families of size 1, representing isolated TFs. The size distribution in Fig. 2 is the observable that we aim to explain in terms of a simple evolutionary model.

Due to the organization of the CIS-BP database, the TF-TF links that we find with our procedure are mainly due to the “inferred” TF-PWM associations of the CIS-BP database, and thus are related to the level of homology between the DBDs of the two TFs. The main assumption of the CIS-BP inference procedure (and thus of the motif family definition) is that high levels of DBD homology should imply high similarity of the corresponding PWMs. In order to assess the robustness of our construction with respect to this assumption, we tested how much the proposed motif families organization would be affected by the inclusion of additional links between TFs on the basis of a direct measure of similarity between their PWMs. The procedure for this robustness test is explained in detail in Section 6 of the Supplementary Material. The Jaccard index can be used as a measure of similarity between each pair of PWMs<sup>29</sup> and thus indirectly between the binding preferences of the corresponding TFs. The TF-TF network defined above can thus be expanded by progressively adding links as the critical threshold for this similarity index is lowered. It turns out that most of the new links coincide with already existing ones or simply join TFs already belonging to the same motif family. Only when the thresholds of similarity between PWM approaches really low values, links connecting TFs belonging to different families start to appear. This result shows the close link between DBD homology and PWM similarity, and supports the robustness of the motif family organization used here.

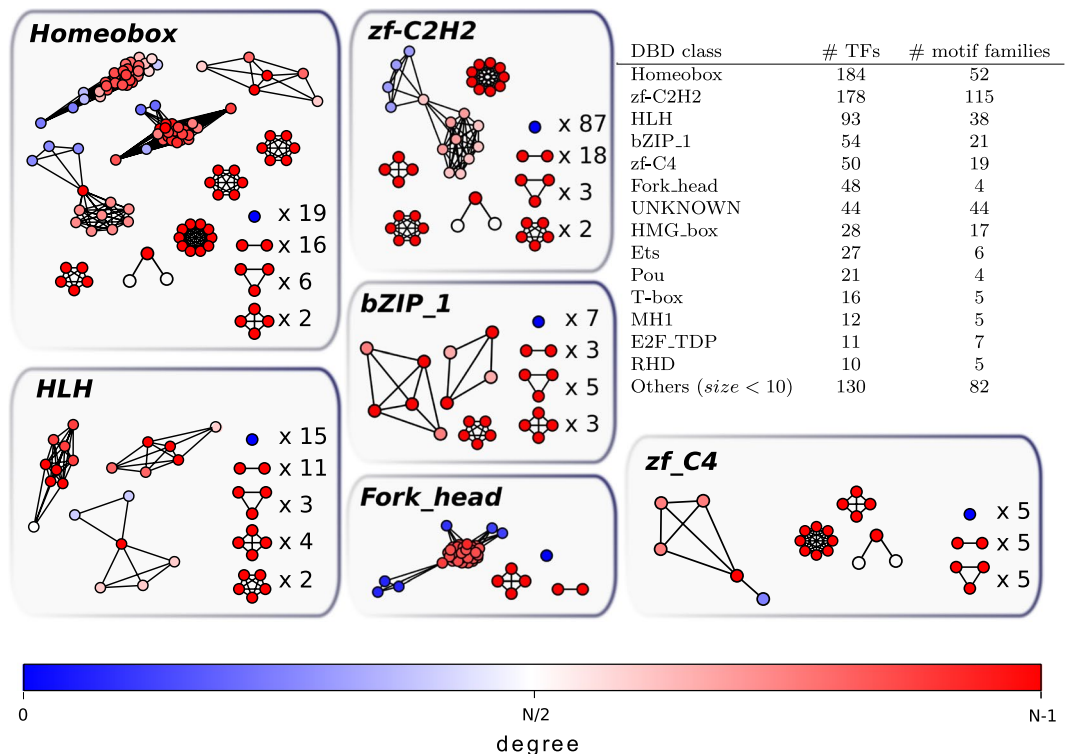


**Figure 1.** Graphical representation of motif families. The table summarizes the organization of the DBD families in motif families. Each vertex is a transcription factor, while links connect two TFs if they share at least one Position Weight Matrix ID. Colors identify the node degree with a color code (reported in the legend) spanning from blue, corresponding to degree 0 (isolated nodes), to red, corresponding to the maximal degree, i.e., the vertex is connected to all other nodes in the family. The circular layout highlights those families that are cliques. See Supplementary Material for reference to detailed family composition.

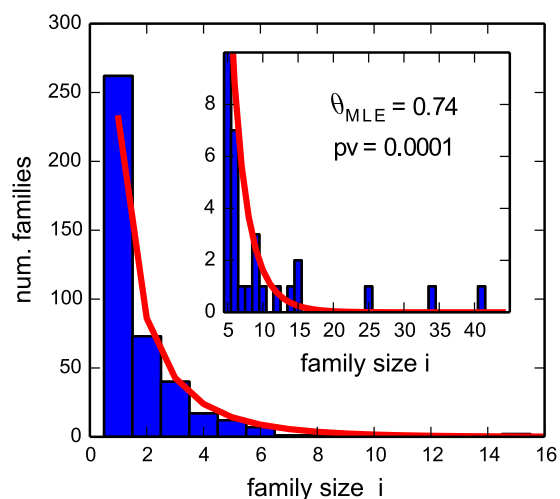


**Figure 2.** Size distribution of motif families in human. The distribution accounts for 906 human TFs, organized in 424 families whose members share at least one PWM with at least another member. The inset is a zoom on the range of sizes  $> 5$ . The red-line is the best-fit model according to maximum likelihood estimation, which has a goodness-of-fit p-value  $p < 0.0001$ . The model captures the general trend, but clearly underestimates the number of families of size 1 and does not predict the presence of the largest families.

**The Birth-Death-*cis*-Innovation model.** The model we propose belongs to the general class of Birth-Death-Innovation models (for a thorough introduction see ref. 30). The focus of these models is on systems in which individual elements are grouped into families whose evolution is ruled by the dynamics of their

individual members. These models typically include the elementary processes of family growth via element duplication (gene duplication), element deletion as a result of inactivation or loss (negative gene mutation), and innovation or emergence of a new family (neutral/positive gene mutation). All these processes are assumed to be of Markov type and the corresponding rates are assumed to be constant in time.

It can be argued that the total number of TFs has been tuned to an optimal one to address in the most efficient way the regulatory needs of the organism. In fact, it has been observed that an upper bound must exist on the total number of TFs to ensure an optimal coding strategy in which misrecognition errors are minimized<sup>31</sup>. Since we aim to describe only the evolution of the TF regulatory strategies in complex eukaryotes, we shall assume that the mean number of TFs is essentially constant over time and stably close to the optimal value. In fact, the dynamics in which we are interested in is the evolution of the binding preferences of these TFs, which is presumably acting on a faster timescale with respect to the changes in the TF total number. This assumption of a separation of time scales is in line with the notion of punctuated equilibrium often implied in several evolutionary models<sup>32</sup>: long period of stasis are punctuated by short bursts of evolutionary activity that involve radical alterations of the duplication and elimination rates. Between these periods of drastic changes, the system seems to rapidly relax to equilibrium. The assumption of equilibrium justifies the assumptions of rates constant in time and an approximate balance between the mechanisms generating an inflow and an outflow of genes, so that the total number of TFs stays constant by mean.

We introduce the dynamic of cis-innovation that makes a TF become the seed of a new family. Given that the repertoire of DBDs in higher eukaryotes is remarkably conserved over the last 600 million years, cis-innovation stands as the driving force of TF innovation on the time scale of PWM evolution we are interested in. In fact, our model description focuses only on the “late” stage of TF evolution in metazoans, in which very few new DBDs, and thus new motif families, are created *de novo*.

In conclusion, we shall evaluate the family size distribution as the stationary state of a process of duplication, deletion and divergence, where the total number of TFs is essentially stable. To introduce the model in more detail, let us define as “class  $i$ ” the set of all families of size  $i$ . Let  $f_i$  be the number of families in the  $i$ -th class,  $M$  be the total number of classes  $i = 1 \dots M$  (or the maximum size of a family), and  $N$  the total number of elements, thus representing also the extreme value for  $M$ . Acting at the “local” level on individual elements, the evolutionary dynamics shapes “globally” the system relocating a family from class  $i$  to class  $i + 1$  in case of duplication (or to class  $i - 1$  in case of removal). Typically, BDI models<sup>33–35</sup> introduce innovation in the model only as a constant inflow in the class 1 due to *de novo* emergence of a new family (increase of  $f_1$  by 1). As discussed above, we propose a generalization of the model by introducing also cis-innovation, in which an element of a family in class  $i$  mutates and gives rise to a new family. This results in the relocation of that element in class 1 and of its original family in class  $i - 1$  (i.e. a decrease of  $f_i$  and increase of  $f_{i-1}$  and  $f_1$  by 1). Let  $\lambda$ ,  $\nu$  and  $\mu$  be the rates of element birth, death, *de novo*-innovation and *cis*-innovation respectively. Solving the master equations at the steady state (see the Materials and Methods section) one finds:

$$f_i = \frac{\nu + \mu N \theta^i}{\lambda} \frac{\theta^i}{i}, \quad (1)$$

where  $\theta = \frac{\lambda}{\delta + \mu}$ .

The corresponding probability distribution  $p_i$  can be found straightforwardly by normalization:

$$p_i = \frac{f_i}{\sum_i f_i} = \frac{1}{\sum_i \frac{\theta^i}{i}} \frac{\theta^i}{i}. \quad (2)$$

A few comments are in order at this point:

- The normalized solution in Equation 2 gives a one-parameter prediction of the size distribution of motif families. The functional dependence on  $\theta$  is equivalent to the one that can be obtained with standard BDI models<sup>30</sup>, i.e., with *de novo* innovation as the only source of innovation. However, our generalized model suggests a different interpretation of the parameter. In fact,  $\theta = \frac{\lambda}{\delta + \mu}$  and thus its value depends on the rate of *cis*-innovation.
- The steady state condition is  $\frac{df_i}{dt} = 0 \forall i$ , implies that the total number of elements  $N = \sum_i^M i f_i$  is constant over time. This condition translates into the parameter constraint  $N(\delta - \lambda) = \nu$ .
- As previously discussed, we expect  $\nu$  to be very small in our case (i.e., negligible *de novo* innovation), and accordingly we shall approximate  $\nu \rightarrow 0$  in the following. We shall further verify “a posteriori” the validity of this approximation using an independent analysis on the evolution of TFs in different lineages (see below). In this regime, the stationary condition simplifies to a balance between duplication and deletion rates  $\lambda = \delta$ , and  $\theta \simeq \frac{1}{1 + \mu/\lambda}$ . Therefore, the deviation of  $\theta$  from 1 allows to directly estimate the magnitude of  $\mu$  with respect to  $\lambda$ , i.e., the relevance of *cis*-innovation with respect to the birth/death rate. As we will see below, a comparison with the data in the human case supports a value of  $\theta \sim 0.73$ , thus highlighting the important role that *cis*-innovation had in the recent evolution of the eukaryotic TF repertoire. Moreover, within this approximation, also the family distribution in Equation 1 can be written in a very simple and compact form:

$$f_i = N \frac{\mu}{\lambda} \left( \frac{\lambda}{\delta + \mu} \right)^i \frac{1}{i} = N(1 - \theta) \frac{\theta^{i-1}}{i}. \quad (3)$$

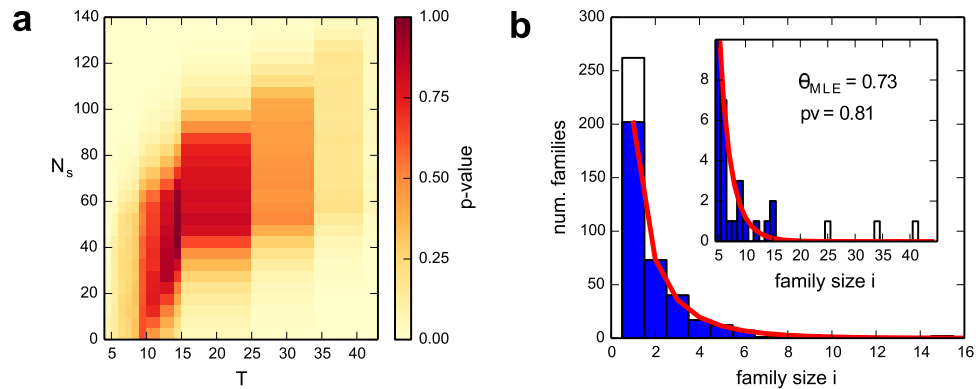


**Figure 3.** (a) Heatmap for the goodness-of-fit p-value as the data sample is reduced. On the x-axis,  $T$  indicates the threshold in size above which families are excluded from the sample. On y-axis  $N_s$  indicates the number of families of size one excluded from the sample. An increase in  $T$  or  $N_s$  reduces the sample size in analysis by reducing the number of TFs considered. For each sample size a goodness-of-fit test for the best-fit model was performed and the corresponding p-value is reported with the color code in the legend. Considering a p-value of 0.75 as the acceptance limit identifies  $T=25$  as the size threshold at which the fit is acceptable. This corresponds to the exclusion of the three largest families. For such a threshold  $T$ , the optimal values for the p-value are reached for values of  $N_s$  in the range  $40 < N_s < 80$ . (b) Size distribution of motif families for the reduced sample. The filled distribution represents the motif family size distribution for the reduced dataset, while the original empirical distribution of Fig. 2 is reported with the unfilled bars. The inset shows a zoom on the range of sizes  $>5$ . The line represents the prediction of our model with the best fit choice of the parameter  $\theta$ , which turns out to fit very well the data contained in the reduced sample with a goodness of fit p-value  $p \sim 0.8$ . The best fit value  $\theta = 0.73$  does not differ substantially from the value that is obtained by fitting the whole empirical sample as in Fig. 2.

- An analytical estimate of the number of classes  $F = \sum_i^M f_i$  in which the  $N$  elements are organized when the dynamics reaches equilibrium can also be calculated as:

$$\frac{F}{N} = \frac{1 - \theta}{\theta} \sum_i^M \frac{\theta^i}{i} \simeq \frac{\theta - 1}{\theta} \ln(1 - \theta) \quad (4)$$

This represents the neutral model prediction on the number of motif families given a set of  $N$  TFs subjected to the described BDI dynamics.

### The model can explain the core of the size distribution of motif families and identifies two main deviations.

The distribution predicted by our neutral evolutionary model (Equation 2) can be compared with the empirical TF organization in motif families. The procedure to extract this empirical distribution is explained in the Materials and Methods section in detail. This comparison can be quantified by estimating the best fit value of the parameter  $\theta$  with a Maximum Likelihood method and a p-value associated to the quality of the fit using a *goodness-of-fit* test based on the Kolmogorov-Smirnov statistics (Materials and Methods). Although the central part of the size distribution seems well captured by the theoretical model, a direct fit of the whole distribution gives very low p-values (p-value  $< 10^{-3}$ , see Fig. 2). This poor p-value shows the presence of significant deviations with respect to our random null-model. These deviations can be easily identified looking at Fig. 2. They are located at the two ends of the distribution and involve a few of the largest families and the smallest ones (i.e., families of size 1). Using the KS test and a p-value threshold for acceptance of 0.75, we can identify in a quantitatively and consistent way the fraction (about 25%) of isolated TFs and the number (three) of the largest families which account for most of the deviations from the null model (Materials and Methods and Fig. 3).

If we subtract from the whole distribution these two tails (for a total of  $\sim 150$  TFs, i.e. about 16% of the total number of TFs in analysis), we eventually find a remarkable agreement between the model predictions and experimental data (p-value  $\sim 0.8$ , see Fig. 3). Therefore, the “core” of the distribution is well described by the exponential-like solution of Eq. (3), while deviations are due to few families that can be isolated and studied in detail. This suggests that the evolution of a large portion of the TF repertoire in higher eukaryotes was driven by a neutral stochastic process of the BDI type with only two exceptions: an excess of isolated TFs and three large families which on the contrary are characterized by a strong level of duplication without innovation. Let us address in more detail these two deviations.

**Single copy transcription factors.** The fitting procedure allows us to obtain a rough estimate of the fraction  $N_s$  of size 1 families which are not explained by our theoretical description. This number is in the range  $40 < N_s < 80$ , i.e. in between 20% and 30% of the total number of size 1 families (Materials and Methods and Fig. 3). The emergence of a size 1 family in our model description can come from *de novo* innovation or from duplication of an existing TF, followed by a *cis*-innovation event that defines a new PWM. We argued that *de novo* innovation is

negligible in our case of study, so we expect that most of the isolated TFs are the result of a previous duplication event. In this scenario, they should share their DBD at least with the TF they duplicated from, and we verified that indeed empirically this is the case for the majority of isolated TFs, thus supporting our model description. However, some isolated TFs have a DBD which is not shared with any other TF (12 in our sample) or are characterized by a DBD which is classified as ‘UNKNOWN’ (44 in our sample), so also potentially unique. The presence of these isolated TFs with unique DBDs can be explained by the two following mechanisms.

**Newly acquired DBDs.** A few of them are due to actual recent de novo innovation events, thus introducing new DBDs in the last period of post-metazoan evolution. These “recent” TFs appear in our analysis most likely as size 1 families only because they had not time to enter into the duplication process. Looking at the orthology maps we can rather easily identify these DBDs and the corresponding TFs (see Supplementary Material and below) which turn out to be very few, thus supporting “a posteriori” our  $\nu = 0$  approximation.

**Singleton genes.** The majority of excess isolated TFs are most probably *singleton genes* for which duplication is peculiarly avoided. The existence of this class of genes has been recently proposed<sup>36,37</sup>. They are supposed to be ancestral genes of prokaryotic origin, addressing basilar functions and requiring a fine-tuning of their abundances, thus making their duplication particularly detrimental. They would be the result of a selective pressure to avoid duplication, and thus, by definition, cannot be explained by our neutral model.

Since singleton genes are not included in our model, they are good candidates to explain the excess of isolated TFs in Fig. 2. To distinguish between putative singleton genes and recent genes in the motif families of size 1, we analyzed their evolutionary origin. More specifically, we manually inspected the taxonomic profiles of these 56 TFs in the EggNOG database<sup>38</sup>: 16 of them have a putative origin at the Last Universal Common Ancestor (LUCA), i.e. they are shared among bacteria, archaea and eukarya; 25 are in common among all eukarya, 4 among opisthokonta, 3 among metazoa and 8 have a post-metazoan origin. Therefore, at least 41 of these TFs have a very ancient origin (LUCA + eukarya) and could well be examples of “singleton” TFs, while 8 are instead of very recent origin (post-metazoan, but 4 of them are shared only among euteleostomi) and are thus likely to be “recent” TFs. These recent TFs constitute less than the 1% of our sample, supporting “a posteriori” the  $\nu = 0$  approximation.

To find additional evidence that these 41 ancient TFs can be bona fide “singleton genes”, we queried the NGC5.0 database<sup>39</sup>, which provides information about the gene duplicability for a large set of cancer genes. 14 of our putative singletons are present in this collection, and 12 of them show indeed no evidence of duplicability (at 60% coverage), thus supporting their “singleton” nature. It is interesting to notice that the overall number of putative singletons (41 genes) is compatible to the size of the deviation from the random null model ( $40 < N_s < 80$ ) observed in our best fit tests. An example of a DBD family (the IRF family) giving rise to a set of motif families of size 1 is discussed in detail in the Supplementary Material (Section 5).

**Over-expanded families.** Our analysis singles out also three over-expanded families. The over-expansion can be due to two parallel mechanisms: an enhanced rate of duplication and/or a decreased rate of cis-innovation. Looking at the three over-expanded families, three very homogeneous groups of TFs can be recognized: the FOX family (size 41), the HOX family (size 34) and another homeobox family (size 25). These three families are good examples of the two mechanisms mentioned above. The HOX family contains TFs well known for their role in morphogenesis and animal body development<sup>40</sup>. Also TFs in the other over-expanded homeobox family show enrichments for GO annotations related to *morphogenesis*, *development* and *pattern specification*, as reported in Table 1. These two families may well represent cases of positive selection for duplication and subsequent fixation. Due to their crucial role in morphogenesis, these TFs could have been retained in multiple redundant copies to ensure proper response under radically changing conditions.

The third family, which is the largest one, collects most of the FOX (Forkhead box) TFs present in the sample. TFs belonging to this family are known to be “bispecific”, i.e. they recognize two distinct DNA sequences<sup>41</sup>, and for this reason they play an important and peculiar role in the regulatory network of metazoans<sup>41</sup>. While their over-expansion can be due to positive selection for functional reasons, their unique feature of bispecific binding could suggest that innovation is particularly difficult for these TFs. In fact, bispecificity is likely to impose stronger constraints, from a structural point of view, than those imposed on other TFs. In this perspective, it is interesting to stress the different distribution of Forkhead and Homeobox genes in motif families. Almost all the Forkhead genes are collected in this single large motif family, suggesting no cis-innovation events that would have moved some of these genes in families of other sizes. Only 6 Forkhead TFs are present in other motif families. On the other hand, Homeobox genes, besides the two main families discussed above, are dispersed in several other motif families, thus are associated to a variety of PWMs. This difference suggests that duplication of Homeobox genes has been positively selected at a certain time point probably because of their crucial role in the development of multicellular organisms (see Table 1), but cis-innovation have progressively changed their binding preferences. On the other hand, very few events of cis-innovation are associated to FOX genes that indeed “accumulated” in a single motif family. These interpretations of the possible evolutionary origins of the over-expanded motif families will be addressed in more detail in the next section.

**Phenomenology of the splitting of DBD families in motif families.** So far, we considered the “global” distribution of all TFs in motif families. However it is also interesting to study separately the behaviour of the different DBD families. Each of them can be considered as an independent instance of the evolutionary model described above and it is interesting to see if there are significant deviations for specific DBD families with respect to the null model predictions. Using as input the value  $\theta = 0.74$  obtained by fitting the whole set of TFs we obtain from Equation (4) a parameter-free prediction for the ratio  $F/N$ . To evaluate also the possible variability of this neutral expectation, we ran  $5 \cdot 10^4$  simulations of the model for different system sizes, corresponding to the different numbers of TFs in the DBD families. We report in Fig. 4 the comparison of the model prediction (dashed line) and the results of model simulations (shaded areas represent 1 and 3 standard deviations from the average

GO biological process complete	Fold Enrichment	p-value
embryonic skeletal system development (GO:0048706)	6.92	7.87E-18
skeletal system development (GO:0001501)	4.21	8.44E-15
embryonic skeletal system morphogenesis (GO:0048704)	7.18	1.20E-14
skeletal system morphogenesis (GO:0048705)	5.77	4.29E-14
anterior/posterior pattern specification (GO:0009952)	4.91	2.55E-13
pattern specification process (GO:0007389)	3.10	3.15E-10
regionalization (GO:0003002)	3.35	7.25E-10
embryonic organ morphogenesis (GO:0048562)	3.47	4.71E-08
embryonic morphogenesis (GO:0048598)	2.66	1.83E-06
organ morphogenesis (GO:0009887)	2.25	4.76E-06
chordate embryonic development (GO:0043009)	2.59	7.91E-06
embryo development ending in birth or egg hatching (GO:0009792)	2.58	9.09E-06
embryo development (GO:0009790)	2.10	2.08E-05
embryonic organ development (GO:0048568)	2.65	4.30E-05
anatomical structure morphogenesis (GO:0009653)	1.76	5.73E-05
system development (GO:0048731)	1.43	7.57E-04
anatomical structure development (GO:0048856)	1.33	8.57E-04
multicellular organism development (GO:0007275)	1.36	1.19E-03
animal organ development (GO:0048513)	1.49	1.97E-03
developmental process (GO:0032502)	1.30	2.77E-03
single-multicellular organism process (GO:0044707)	1.32	4.44E-03

**Table 1.** Gene Ontology analysis of the genes belonging to the two homeobox families of size 25 and 34. Only results with p-value below 0.01 are shown. The enriched annotations are mainly associated to development and morphogenesis of multicellular organisms.

simulated behaviour) with empirical data (symbols). While most of the DBD families do not deviate significantly from the model prediction, three clear “outliers” can be observed. The Forkhead and Homeobox DBD families show a smaller than expected number of motif families while the Zinc Finger class of TFs is splitted in more families than expected. These deviations can be traced back to the peculiar features of these DBDs. In the case of the Forkhead TFs the low value of  $F/N$  is likely a consequence of the structural constraints typical of the Forkhead DBD which limit the evolvability of the binding preferences leading to a lower-than-average rate of cis-innovation and thus a smaller number of motif families. For the Homeobox DBD instead there seems to be no structural reason for this “freezing” of motif diversity. It is tempting to speculate that the low value of  $F/N$  is in this case related to the special role played by these genes in the regulatory network. Indeed Hox genes are known to be crucial players of the development of multicellular organisms and it is nice to see how this special role is highlighted by our simple model. The other significant deviation from the model prediction concerns a Zinc Finger class of TFs, that appears to have greatly diversified the TF PWMs. The corresponding motif families are not over-expanded, in fact they did not emerge as deviations in the previous analysis (Fig. 2). In fact, the histogram of their motif family sizes (the analogous of Fig. 2 but restricted to Zinc Finger TFs, see Figure S1) follows reasonably well our null model. However, the fitted parameter  $\theta = 0.56$  is well below the value obtained for all TFs ( $\theta = 0.74$ ), thus confirming again that the rate of cis-innovation for this DBD family is higher than the average rate for all TFs. Zinc Finger TFs are known to be characterized by multiple tandem C2H2 zinc finger domains. Such modularity enabled a rapid functional divergence among recently duplicated paralogs, as each domain in the protein can mutate independently<sup>42</sup>. This structural feature is well represented by our simple model.

**TF redundancy of binding increases with organism complexity.** This section addresses the differences in the motif family organization in different eukaryotic species. In particular, we focused on model species, which are expected to have well annotated TF repertoires. The same type of analysis presented in Fig. 2 was

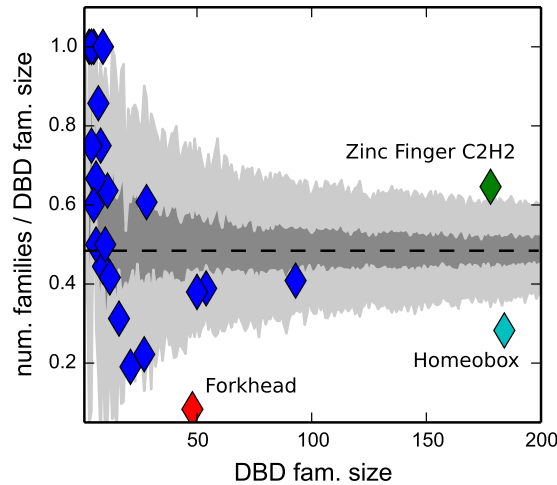


**Figure 4.** Splitting of DBD families in motif families. The ratio  $F/N$  is plotted as a function of the number of TFs of the DBD family. Each point represents the empirical value for a DBD family, while the dashed line represents the expected value for  $\theta = 0.74$  as given by Eq. 4. In order to evaluate the fluctuations on the expectation, we simulated the evolution of  $5 * 10^4$  DBD families, with starting size ranging from 1 to 500,  $\theta = 0.74$  and  $\lambda = \delta$ . The two shaded areas correspond to 1 standard deviation and 3 standard deviations from the average. Green diamond: Zinc Finger C2H2 family. Cyan diamond: Homeobox family. Red diamond: Forkhead family.

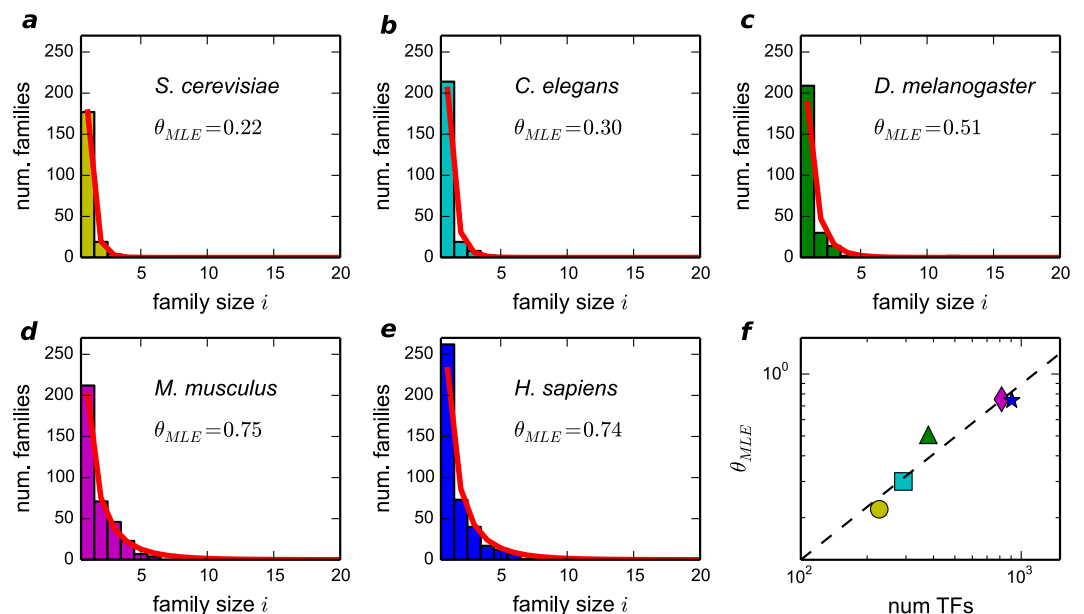


**Figure 5.** Size distribution of TF motif families for different eukaryotic organisms. (a–e) We report the distributions and the best fit values of  $\theta$  for five different organisms of increasing complexity. As for the human case, the data are taken from the CIS-BP database. (f) The bottom-right panel shows how  $\theta$  scales with the number of TFs. The red-line is the fit  $\theta \sim (\# \text{ TFs})^{0.85}$ .

performed on the set of TFs of yeast and of three other species of increasing complexity in the animal lineage: *C. elegans*, *D. melanogaster* and *M. musculus*. Figure 5 shows the histograms of the family size distributions and the corresponding fits with the prediction of the neutral evolutionary model in Equation (2). In all tested cases, the motif families distribution follows the predicted functional form with a level of agreement comparable to the human case discussed above. However, there is a clear trend of the fitted parameter  $\theta$  to increase with complexity as measured by the number of TFs in the species (or alternatively by the total number of genes). This trend is reported in Fig. 5 and it is sublinear in the investigated window of TF repertoires. The definition of  $\theta \simeq \frac{1}{1 + \mu/\lambda}$  indicates that this trend corresponds to a decrease rate of cis-innovation, with respect to the duplication rate, as the complexity of the organism increases.



The value of  $\theta$  intuitively represents the level of “redundancy”, i.e., the tendency of TFs to keep the same binding preferences. Actually, this parameter can be used to quantify the retained redundancy of TF binding in a neutral evolution context: the higher is the  $\theta$  value, the slower is the TF divergence with respect to the duplication rate. The limit value  $\theta = 1$  implies that the distribution in Equation (1) becomes a power-law distribution with motif families. Figure 5 (right-bottom) shows that this level of “redundancy” increases with the organism complexity as measured with the total number of TFs. Note that we tested with extensive simulations that the value of  $\theta$  is not in principle dependent on the total number of TFs (see Figure S2) if the rates are constant. This further confirms that Fig. 5 captures a non trivial trend of the innovation dynamics with genome size.

## Discussion

In this paper we addressed quantitatively the evolutionary dynamics of the transcription factor repertoire. We introduced and discussed a classification that groups the TFs by reason of their binding preferences into what we call motif families. Such an approach is sensitive to a fine divergence in regulation that would have been undetectable using the DBD taxonomy. The evolution of the motif families proves to be well described by a simple neutral model that depends only on one free parameter  $\theta$ . Ultimately  $\theta$  accounts for the relevance of divergence between TFs with respect to retention of redundant copies. It can be seen as a readout of the level of redundancy of TF binding preferences, which reports how much the regulatory system has been shaped by duplication vs innovation.

We devised two main deviations from the neutral scenario that seem to be due to opposite evolutionary pressures. A positively selected over-expansion of some families that are associated to multicellularity evolution. The inhibition of duplication for a specific set of ancient TFs, or “singletons”, that can be traced back to their unicellular ancestors. Looking at the motif family organization allows to tackle the evolution of transcriptional regulation and identify global trends in comparative genomics, since it does not require to know in detail the transcription network, but just the TF binding preferences. Moreover, the parameter  $\theta$  of redundancy grants an easy way to compare different organisms.

A major issue in the study of the evolution of regulatory systems is to identify those features which can be in some way associated to the organism complexity. Combinatorial regulation is a distinctive feature of complex eukaryotes. Indeed, prokaryotic and eukaryotic TFs use different binding strategies, with PWMs of high and low information content respectively<sup>43</sup>. This difference is related to the evolution of the combinatorial strategies of control, typical of higher eukaryotes, that can compensate the low information content of their TF binding sites by combining several of them in the same promoter<sup>43</sup>. This could have also been favoured by the widespread presence of transposable elements able to convey combinations of TF binding sites all over the genome<sup>44</sup>. However, if the PWMs that characterize a motif family have low information content, the set of preferred binding sequences is loosely defined and can include several possible sequences. Thus, the mutation process is less likely to drive a TF away from its motif family. This would translate in a lower cis-innovation rate in our model for organisms with higher complexity, and this trend seems indeed to emerge from our comparison of the different motif family organization in different species (Fig. 5).

The increased degeneracy of TF PWMs can also have another relevant consequence. Having larger motif families enables a different layer of combinatorial regulation, where several redundant TFs compete for the same binding site. In other words, a binding site may be subject to the combinatorial regulation of several TFs as well as a promoter is subject to the combinatorial regulation of several binding sites. Our findings suggest that eukaryotes of increasing complexity do not need only a richer repertoire of TFs to regulate an expanded genome, but also an increased redundancy of TF PWMs. Speculatively, such an increase is aimed at the implementation of this additional layer of combinatorial regulation.

In conclusion, complexity seems to be associated to the redundancy of the TF repertoire, i.e., to the presence of large families of TFs which recognize the same binding sequences. It would be interesting to understand the consequences of this observation on the topology and function of the regulatory network.

## Methods

**Data set.** We took advantage of the Catalog of Inferred Sequence Binding Preferences (CIS-BP database<sup>27</sup>, version number 1.02), which collects the specificities of a vast amount of TFs in several species. The PWMs in this database were either directly derived from systematic protein binding microarray (PBM) experiments or inferred by overall DBD amino acid identity. Furthermore, the CIS-BP database gathers data from all the main existing databases (such as TRANSFAC<sup>45</sup>, JASPAR<sup>46</sup> and SELEX<sup>47</sup>) and several Chip-Seq experiments, which had been used for cross-validation. To construct the motif families, we downloaded the PWMs associated to each TF, considering both those obtained from experimental assays and the inferred ones. In this way, we obtained 4172 PWM unique identifiers (PWD IDs) annotated to 906 different TFs.

**The BDI model.** We define as “class  $i$ ” the set of all families of size  $i$ .  $f_i$  represents the number of families in the  $i$ -th class and  $M$  be the total number of classes  $i = 1 \dots M$  corresponding to the possible family sizes, with  $M$  at most equal to the total number of elements  $N$ .

The evolution equations are:

$$\begin{aligned}\frac{df_1(t)}{dt} &= -(\lambda + \delta + \mu)f_1(t) + 2(\delta + \mu)f_2(t) + \mu N + \nu \\ \frac{df_i(t)}{dt} &= (i-1)\lambda f_{i-1}(t) - i(\lambda + \delta + \mu)f_i(t) + (i+1)(\delta + \mu)f_{i+1}(t) \\ \frac{df_M(t)}{dt} &= (M-1)\lambda f_{M-1}(t) - M(\delta + \mu)f_M(t)\end{aligned}\quad (5)$$

where  $\lambda$ ,  $\delta$ ,  $\nu$  and  $\mu$  denote the birth, death, *de novo* innovation and *cis*-innovation rates respectively.

The model can be mapped in the simplest case of the BDI models discussed in ref. 30 with the substitution  $\delta' = \delta + \mu$  and  $\nu' = \nu + \mu N$ .

From the general solution discussed in ref. 30, we obtain at steady state:

$$f_i = \frac{\nu'}{\lambda} \left( \frac{\lambda}{\delta'} \right)^i \frac{1}{i} \sim \frac{\theta^i}{i} \quad (6)$$

where  $\theta = \frac{\lambda}{\delta'} = \frac{\lambda}{\delta + \mu}$ . If, following<sup>30</sup>, we assume a balance between birth and death rates  $\lambda = \delta$  then  $\theta = \frac{\lambda}{\lambda + \mu}$  and Eq. (6) becomes:

$$f_i = \frac{\nu + \mu N}{\lambda} \left( \frac{\lambda}{\lambda + \mu} \right)^i \frac{1}{i} \quad (7)$$

The deviation of  $\theta$  from 1 allows to estimate the magnitude of  $\mu$  with respect to  $\lambda$ . In the limit of  $\theta \rightarrow 1$  ( $\mu \rightarrow 0$ ) the usual power-like behaviour of the standard DBI model is recovered. Since we know  $\nu \ll \mu$ , we shall assume  $\nu = 0$  and the solution of the model eq. (7) becomes a function only of  $\theta$ .

$$f_i = N \frac{\mu}{\lambda} \left( \frac{\lambda}{\lambda + \mu} \right)^i \frac{1}{i} = N(1 - \theta) \frac{\theta^{i-1}}{i}$$

**Maximum Likelihood estimation of  $\theta$ .** To perform a MLE of the parameter  $\theta$ , we must first move from the distribution of the number of families to a probability distribution. This is simply achieved by normalizing the  $f_i$ :  $p_i = C_M \frac{\theta^i}{i}$ . The normalization constant  $C_M$  assumes a very simple form in the large  $M$  limit:

$$C_M = \left[ \sum_{i=1}^M \frac{\theta^i}{i} \right]^{-1} \stackrel{M \rightarrow \infty}{\approx} [-\ln(1 - \theta)]^{-1},$$

leading to the probability distribution:

$$p_i = \frac{1}{-\ln(1 - \theta)} \frac{\theta^i}{i} \quad (8)$$

We show in the Supplementary Material that for our range of values of  $M$  and  $\theta$  the error induced by this approximation is negligible.

The probability distribution in Eq. 8 is simple enough to allow an analytic determination of the MLE for  $\theta$  (see the Supplementary Material for the detailed calculation), which turns out to be:

$$\theta_{MLE} = 1 - e^{\frac{1}{\bar{k}} + W_{-1}\left(-\frac{1}{\bar{k}} e^{-\frac{1}{\bar{k}}}\right)} \quad (9)$$

where  $\bar{k}$  is the mean size over the sample and  $W$  is the Lambert Function.

**Goodness-of-fit test.** We compared the empirical data with our model, defined by  $\theta_{MLE}$ , following the strategy proposed in ref. 48. More precisely we used the Kolmogorov-Smirnov (KS) statistic as a measure of the distance between the distribution of the empirical data and our model. In order to obtain an unbiased estimate for the p-value, we created a set of one thousand synthetic data samples with the same size of the empirical one, drawn from a distribution with the same  $\theta_{MLE}$  value. For each synthetic sample, we computed the KS statistic relative to the best-fit law for that set and constructed the distribution of KS values. The p-values reported in the paper represent the fraction of the synthetic distances larger than the empirical one.

**Gene Ontology.** We performed a gene ontology analysis on the genes belonging to the union of the three larger motif families using the over-representation test of the PANTHER facility<sup>49</sup> and selecting only the Biological Process ontology. We chose as a background for the test the entire data sample (906 TFs) to eliminate annotations simply associated to generic regulatory functions of TFs. p-values were evaluated using the Bonferroni correction.

## References

- Accili, D. & Arden, K. C. Foxos at the crossroads of cellular metabolism, differentiation, and transformation. *Cell* **117**, 421–426 (2004).
- Bain, G. *et al.* E2a proteins are required for proper b cell development and initiation of immunoglobulin gene rearrangements. *Cell* **79**, 885–892 (1994).
- Dynlacht, B. D. Regulation of transcription by proteins that control the cell cycle. *Nature* **389**, 149–152 (1997).
- Furney, S. J., Higgins, D. G., Ouzounis, C. A. & López-Bigas, N. Structural and functional properties of genes involved in human cancer. *BMC Genomics* **7**, 3 (2006).
- Bustamante, C. D. *et al.* Natural selection on protein-coding genes in the human genome. *Nature* **437**, 1153–1157 (2005).
- De, S., Lopez-Bigas, N. & Teichmann, S. A. Patterns of evolutionary constraints on genes in humans. *BMC Evol. Biol.* **8**, 275 (2008).
- Lopez-Bigas, N., De, S. & Teichmann, S. A. Functional protein divergence in the evolution of homo sapiens. *Genome Biol* **9**, R33 (2008).
- Voordeckers, K., Pougach, K. & Verstrepen, K. J. How do regulatory networks evolve and expand throughout evolution? *Current Opinion in Biotechnology* **34**, 180–188 (2015).
- Teichmann, S. A. & Babu, M. M. Gene regulatory network growth by duplication. *Nature genetics* **36**, 492–496 (2004).
- Madan Babu, M., Teichmann, S. A. & Aravind, L. Evolutionary dynamics of prokaryotic transcriptional regulatory networks. *J. Mol. Biol.* **358**, 614–33 (2006).
- Cordero, O. X. & Hogeweg, P. Feed-forward loop circuits as a side effect of genome evolution. *Molecular biology and evolution* **23**, 1931–6 (2006).
- Enemark, J. & Sneppen, K. Gene duplication models for directed networks with limits on growth. *Journal of Statistical Mechanics: Theory and Experiment* **2007**, P11007–P11007 (2007).
- Pinney, J. W., Amoutzias, G. D., Rattray, M. & Robertson, D. L. Reconstruction of ancestral protein interaction networks for the bzip transcription factors. *Proc. Natl. Acad. Sci. USA* **104**, 20449–53 (2007).
- Aldana, M., Balleza, E., Kauffman, S. & Resendiz, O. Robustness and evolvability in genetic regulatory networks. *Journal of theoretical biology* **245**, 433–48 (2007).
- Crombach, A. & Hogeweg, P. Evolution of evolvability in gene regulatory networks. *PLoS Comput. Biol.* **4**, e1000112 (2008).
- Nowick, K. & Stubbs, L. Lineage-specific transcription factors and the evolution of gene regulatory networks. *Briefings in functional genomics* **9**, 65–78 (2010).
- Ohno, S. *Evolution by gene duplication* (Springer, 1970).
- Zhang, J. Evolution by gene duplication: an update. *Trends in Ecology & Evolution* **18**, 292–298 (2003).
- Demuth, J. P. & Hahn, M. W. The life and death of gene families. *Bioessays* **31**, 29–39 (2009).
- Conant, G. C. & Wolfe, K. H. Turning a hobby into a job: How duplicated genes find new functions. *Nature Reviews Genetics* **9**, 938–950 (2008).
- Lynch, M. & Conery, J. S. The evolutionary fate and consequences of duplicate genes. *Science* **290**, 1151–1155 (2000).
- Britten, R. J. Divergence between samples of chimpanzee and human DNA sequences is 5%, counting indels. *Proceedings of the National Academy of Sciences* **99**, 13633–13635 (2002).
- Cheng, Z. *et al.* A genome-wide comparison of recent chimpanzee and human segmental duplications. *Nature* **437**, 88–93 (2005).
- Perez, J. C. *et al.* How duplicated transcription regulators can diversify to govern the expression of nonoverlapping sets of genes. *Genes & Development* **28**, 1272–1277 (2014).
- Gu, Z. *et al.* Role of duplicate genes in genetic robustness against null mutations. *Nature* **421**, 63–66 (2003).
- Baker, C. R., Hanson-Smith, V. & Johnson, A. D. Following gene duplication, paralogue interference constrains transcriptional circuit evolution. *Science* **342**, 104–108 (2013).
- Weirauch, M. T. *et al.* Determination and inference of eukaryotic transcription factor sequence specificity. *Cell* **158**, 1431–1443 (2014).
- Jolma, A. *et al.* Dna-binding specificities of human transcription factors. *Cell* **152**, 327–339 (2013).
- Vorontsov, I. E., Kulakovskiy, I. V. & Makeev, V. J. Jaccard index based similarity measure to compare transcription factor binding site models. *Algorithms for Molecular Biology* **8**, 23 (2013).
- Karev, G. P., Wolf, Y. I., Rzhetsky, A. Y., Berezhovskaya, F. S. & Koonin, E. V. Birth and death of protein domains: a simple model of evolution explains power law behavior. *BMC Evol. Biol.* **2**, 18 (2002).
- Itzkovitz, S., Tlusty, T. & Alon, U. Coding limits on the number of transcription factors. *BMC genomics* **7**, 239 (2006).
- Koonin, E. V., Wolf, Y. I. & Karev, G. P. The structure of the protein universe and genome evolution. *Nature* **420**, 218–223 (2002).
- Novozhilov, A. S., Karev, G. P. & Koonin, E. V. Biological applications of the theory of birth-and-death processes. *Briefings in bioinformatics* **7**, 70–85 (2006).
- Fenner, T., Levene, M. & Loizou, G. A stochastic evolutionary model exhibiting power-law behaviour with an exponential cutoff. *Physica A: Statistical Mechanics and its Applications* **355**, 641–656 (2005).
- Lagomarsino, M. C., Sellerio, A. L., Heijning, P. D. & Bassetti, B. Universal features in the genome-level evolution of protein domains. *Genome biology* **10**, 1–13 (2009).
- Carroll, S. B. Evo-devo and an expanding evolutionary synthesis: a genetic theory of morphological evolution. *Cell* **134**, 25–36 (2008).
- D'Antonio, M. & Ciccarelli, F. D. Modification of gene duplicability during the evolution of protein interaction network. *PLoS Comput. Biol.* **7**, e1002029 (2011).
- Huerta-Cepas, J. *et al.* eggNOG 4.5: a hierarchical orthology framework with improved functional annotations for eukaryotic, prokaryotic and viral sequences. *Nucleic Acids Res.* **44**, D286–D293 (2016).
- An, O., Dall'Olivo, G. M., Mourikis, T. P. & Ciccarelli, F. D. Ncg 5.0: updates of a manually curated repository of cancer genes and associated properties from cancer mutational screenings. *Nucleic Acids Res.* **44**, D992–D999 (2016).
- Pavlopoulos, A. & Akam, M. Hox go omics: insights from drosophila into hox gene targets. *Genome Biol* **8**, 208 (2007).
- Nakagawa, S., Gisselbrecht, S. S., Rogers, J. M., Hartl, D. L. & Bulyk, M. L. Dna-binding specificity changes in the evolution of forkhead transcription factors. *Proceedings of the National Academy of Sciences* **110**, 12349–12354 (2013).
- Emerson, R. O. & Thomas, J. H. Adaptive evolution in zinc finger transcription factors. *PLoS Genet* **5**, e1000325 (2009).
- Wunderlich, Z. & Mirny, L. A. Different gene regulation strategies revealed by analysis of binding motifs. *Trends Genet.* **25**, 434–440 (2009).
- Testori, A. *et al.* The role of transposable elements in shaping the combinatorial interaction of transcription factors. *BMC genomics* **13**, 400 (2012).
- Matys, V. *et al.* Transfac and its module transcompel: transcriptional gene regulation in eukaryotes. *Nucleic Acids Res.* **34**, D108–D110 (2006).
- Mathelier, A. *et al.* Jasp 2014: an extensively expanded and updated open-access database of transcription factor binding profiles. *Nucleic Acids Res.* **42**, D142–D147 (2014).
- Jolma, A. *et al.* Multiplexed massively parallel selex for characterization of human transcription factor binding specificities. *Genome research* **20**, 861–873 (2010).
- Clauset, A., Shalizi, C. R. & Newman, M. E. Power-law distributions in empirical data. *SIAM review* **51**, 661–703 (2009).
- Mi, H., Muruganujan, A. & Thomas, P. D. Panther in 2013: modeling the evolution of gene function, and other gene attributes, in the context of phylogenetic trees. *Nucleic Acids Res.* **41**, D377–D386 (2013).

## Acknowledgements

We thank F.D. Cicarelli and M. Cosentino Lagomarsino for critical reading of the manuscript, and A. Colliva, M. Fumagalli and A. Mazzolini for useful discussions. The work was partially supported by the Compagnia San Paolo grant GeneRNet.

## Author Contributions

M.C. conceived the project; A.R., M.O. and M.C. analysed the data and developed the model. A.C. built and analysed the motif network based on PWMs. All authors wrote and reviewed the manuscript.

## Additional Information

**Supplementary information** accompanies this paper at doi:[10.1038/s41598-017-07761-0](https://doi.org/10.1038/s41598-017-07761-0)

**Competing Interests:** The authors declare that they have no competing interests.

**Publisher's note:** Springer Nature remains neutral with regard to jurisdictional claims in published maps and institutional affiliations.



**Open Access** This article is licensed under a Creative Commons Attribution 4.0 International License, which permits use, sharing, adaptation, distribution and reproduction in any medium or format, as long as you give appropriate credit to the original author(s) and the source, provide a link to the Creative Commons license, and indicate if changes were made. The images or other third party material in this article are included in the article's Creative Commons license, unless indicated otherwise in a credit line to the material. If material is not included in the article's Creative Commons license and your intended use is not permitted by statutory regulation or exceeds the permitted use, you will need to obtain permission directly from the copyright holder. To view a copy of this license, visit <http://creativecommons.org/licenses/by/4.0/>.

© The Author(s) 2017